# Influence of adsorption and diffusion rates on the growth of $Pb_{1-x}Fe_xS$ nanoparticle films

Varsha Banerjee,* Rakesh K. Joshi, and H. K. Sehgal
*Department of Physics, Indian Institute of Technology, Hauz Khas, New Delhi 110016, India*
(Received 7 January 2004; revised manuscript received 15 July 2004; published 29 September 2004)

We study the effect of adsorption rate on the particle size distribution in solution-grown ternary $Pb_{1-x}Fe_xS$ nanoparticle films. Computer simulations of a stochastic lattice model with adsorption and mass dependent diffusion have been performed to mimic the underlying mechanism of particle growth. The experimental as well as numerical data exhibit identical scaling with respect to the incident flux rate. A transmission electron microscope analysis of $Pb_{1-x}Fe_xS$ nanoparticle films reveals self-similarity in the particle size distributions corresponding to different adsorption rates as a manifestation of the observed scaling.

DOI: 10.1103/PhysRevE.70.036122 PACS number(s): 89.75.Da

## I. INTRODUCTION

Of late, considerable experimental and theoretical efforts are being made to understand the process of nucleation and growth in the production of thin films; high quality crystals, and nanostructures [1–5]. A large number of experimental techniques have evolved in which atoms deposited on a substrate diffuse and aggregate to form a distribution of islands of various sizes [4,6]. The diffusion processes across the substrate control the mobility and overall kinetics of the nonequilibrium growth process. The incident flux and substrate temperature are the other crucial factors which govern the quality and morphology of the growth process.

On the microscopic scale, the fate of an adsorbed particle, as revealed by atomic scale measurements such as scanning tunneling microscopy (STM), reflection high energy electron diffraction, and transmission electron microscopy (TEM), could be to find one or more diffusing particles and nucleate to form a new island or to find an existing island, get incorporated, and help in the growth of the island [7–10]. Not only small groups of particles but large islands containing several hundred particles have also been found to be mobile, but with a lower mobility [11–14]. Further, recent STM measurements at near room temperature have revealed that the rate of escape of a particle from an island is negligible compared to the rate of surface diffusion thus making aggregation an irreversible process [8,9]. These observations have given an impetus to theoretical modeling incorporating the above microscopic mechanisms to study surface growth [15–21]. The resulting morphology and spatial distribution of the ever-evolving islands is a topic of great contemporary interest.

In this paper, we study the mechanism of growth in solution-grown ternary $Pb_{1-x}Fe_xS$ semiconducting nanoparticle films by numerical simulations of a stochastic lattice model, incorporating just the basic mechanisms of single particle adsorption, mass dependent diffusion, and aggregation. We observe a scaling of the particle size distribution with respect to the deposition rate in the experimental as well as numerical data. The observed scaling is interpreted in terms of self-similarity of the growth process by utilizing TEM data corresponding to $Pb_{1-x}Fe_xS$ films for different deposition rates.

On the practical side, there is a growing interest in the synthesis of semiconducting nanoparticles due to the sensitivity of their physical and chemical properties to size [22]. For example, bulk lead sulfide (PbS) is a *p*-type semiconductor with an optical band gap of 0.41 eV. However, an increase in band gap from 0.41 to 5.4 eV is observed as the crystallite size is reduced from 20 to 2 nm [23,24]. In ternary semiconductors, the band gap and hence the optical properties can also be tailored by varying material composition. Iron sulfide (FeS) has a hexagonal structure with an energy gap of 0.04 eV in the bulk phase and *p*-type conduction. When mixed with PbS, the resulting bulk $Pb_{1-x}Fe_xS$ ternary alloys are likely to have energy band gap values between 0.04 and 0.41 eV. A composition dependence of optical and electrical properties has indeed been observed in $Pb_{1-x}Fe_xS$ nanoparticle films [25]. Thus, the possibility of tuning these properties by controlling size and material composition makes ternary semiconductors interesting candidates for optoelectronic devices.

The paper is organized as follows. The experimental technique describing the procedure for obtaining $Pb_{1-x}Fe_xS$ nanoparticle films is described in Sec. II. The details of the adsorption-diffusion model are presented in Sec. III. Experimental results, their comparison with corresponding numerical data, and discussions follow in Sec. IV. A short conclusion is provided in Sec. V.

## II. EXPERIMENTAL TECHNIQUE FOR $Pb_{1-x}Fe_xS$ NANOPARTICLE FILMS

In our experiments, the nanoparticle films were deposited by a chemical bath deposition (CBD) method which involves a controlled growth of $Pb_{1-x}Fe_xS$ nanoparticles on a suitable substrate [25]. A typical medium in the CBD process consists of one or more metal salts, a source for the chalcogenide *X* (=S,Te,Se) and a chelating agent to limit the hydrolysis of the metal ion and impart some stability to the bath which would otherwise undergo rapid hydrolysis and precipitation. The distinct advantages of this method over alternative tech-

*Corresponding author.
Email address: varsha@physics.iitd.ernet.in

 

niques are its simplicity and relatively low capital expenditures for large area depositions.

Aqueous solutions of $(M/25)$ lead acetate, $(M/25)$ ferrous chloride, and $(M/20)$ thiourea prepared using analytical grade chemicals and deionized water were used to obtain ternary $Pb_{1-x}Fe_{0.5}S$ semiconductor films on cleaned silicon substrates. The high dilutions resulted in a slow growth rate, providing control over the quality of the films. The chemical bath was maintained at a temperature of 30°C was stirred continuously. Optimized quantities of precursors to achieve a specific composition of $x$ were obtained by analyzing x-ray fluorescence data from test films grown under identical conditions. The rate of deposition of $Pb_{1-x}Fe_xS$ particles was controlled by the availability of $S^{2-}$ ions produced by the hydrolysis of thiourea in the basic medium. The increase in deposition rate was achieved by increasing the $p$H of the chemical bath by addition of liquor ammonia which provided excess $(OH^-)$ ions for enhanced hydrolysis of thiourea. Thus increasing the $p$H of the chemical bath led to an increase in the flux of the impinging particles on the substrate, which further led to an enhanced growth of $Pb_{1-x}Fe_xS$ nanoparticles. The involved chemistry is encapsulated in the equation

$$(1-x)Pb(CH_3COO)_2 + xFeCl_2 + (NH_2)_2CS \xrightarrow{NH_4OH} Pb_{1-x}Fe_xS + CH_3COOH + NH_4Cl.$$

Films with different values of $p$H of the chemical bath were grown for optimized times to obtain a thickness of approximately 30 nm. Information about the particle size distributions of the deposited films was obtained by a TEM analysis in a plane-view mode using a Philips CM20 instrument.

### III. THE AGGREGATION-DIFFUSION MODEL

The theoretical description of nonequilibrium growth is known to be a very difficult problem. It is therefore not surprising that a substantial part of our knowledge about such phenomena stems from numerical simulation studies of a wide variety of adsorption-diffusion models.

Our simulations to mimic the growth process of $Pb_{1-x}Fe_xS$ are based on a simple stochastic lattice model which assumes particles to be pointlike, yielding point islands. The mass at a site is thus a reflection of the particle size during the growth process. A lot of theoretical insight supported by numerics into the mass distributions for a variety of aggregation-diffusion stochastic lattice models with point particles has been provided in Refs. [26,27]. These models are known to be relatively simple to implement computationally. It is also known that the simulations of the point particle models directly correspond to the Smoluchowski rate equations which provide an alternative approach to analyze surface growth [19,20].

We incorporate just the basic moves corresponding to adsorption and diffusion and aggregation. The starting point is a two-dimensional discrete lattice with periodic boundary conditions. Each site of the lattice has a mass variable $m_{i,j}$ associated with it. We choose the initial state as an empty lattice; thus $m_{i,j}=0$. A unit integer mass is then dropped at a randomly chosen site $(i,j)$ and the dynamic evolution of the system proceeds according to one of the following microscopic moves.

(1) *Adsorption*. With probability $P_a=F/(1+F)$, a single particle is adsorbed at site $(i,j)$; thus $m_{i,j}\rightarrow m_{i,j}+1$.

(2) *Diffusion and aggregation*. With probability $P_d=1/(1+F)$, diffusion could happen with a probability $D(m)=m^{-\gamma}$. Thus mass $m_{i,j}$ at site $(i,j)$ moves to one of the four nearest neighbor sites, viz., $(i-1,j)$, $(i+1,j)$, $(i,j-1)$, or $(i,j+1)$, chosen at random. If the mass moves to a site which has already some particles, then the total mass just adds up. Thus $m_{i,j}\rightarrow 0$ and $m_{i\pm1,j\pm1}\rightarrow m_{i\pm1,j\pm1}+m_{i,j}$.

(3) If the site chosen is empty, only adsorption can occur with a probability $F/(1+F)$.

The flux rate $F$ in the simulation may be identified with the $p$H of the chemical bath in $Pb_{1-x}Fe_xS$ nanoparticle depositions, recalling that the role of the latter is to provide stable nuclei for deposition on the substrate. While the second move tends to create big masses via diffusion and aggregation in addition to vacant sites, the first move replenishes the lower end of the mass spectrum. It is thus expected that the evolution of the mass distribution over the two-dimensional substrate will be influenced by these two competing mechanisms.

A few remarks regarding our choice of a mass dependent diffusion term are in order. It stems from experimental support obtained from time sequenced STM measurements performed over a variety of nanoparticle films obtained using epitaxtial techniques [11–14]. In these papers, a STM image of a spot yielded information about the position, size, and shape of the two-dimensional compact islands in that region. The structures were then followed quantitatively as a function of time over a period of several hours. Having established that the islands diffuse, the diffusibility was calculated from the mean square displacement of the islands over the observation time. An unambiguous experimental evidence of mass dependent diffusion of the form $D\sim m^{-\gamma}$ was established for clusters comprised of approximately 100 particles or less. While large clusters were also found to undergo measurable diffusion, they did not seem to show any such systematic variation with $m$ [11].

Some comments on the diffusion parameter $\gamma$ are also in order. $\gamma=0$ corresponds to mass independent diffusion implying that clusters of all sizes are equally mobile. On the other hand, if $\gamma$ is sufficiently large, only small groups of particles are mobile. Thus $\gamma$ is expected to play a crucial role in the distribution of masses over the two-dimensional substrate. Its numerical value as expected depends on the physical and chemical properties of the incident particles as well as the ambient temperature [12,14,28].

A large number of similar cluster-cluster aggregation (OCA) models have been extensively studied to understand the kinetics of nonequilibrium surface growth. Excellent reviews can be found in the books by Vicsek and Family [2,3]. We mention briefly a few which are of direct relevance to the present work. The starting point of a typical CCA model is a two-dimensional square lattice with a small fraction of ran-

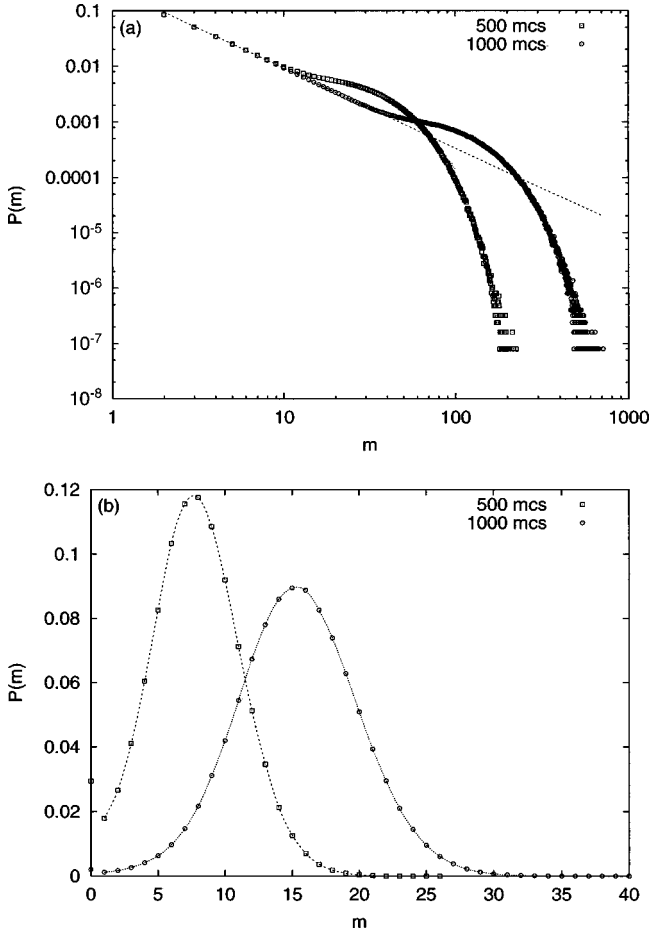


FIG. 1. Mass distribution $P(m)$ obtained from the simulation of the model of Sec. III on a lattice of size $250\times250$ for the diffusion parameter $\gamma$ equal to (a) 0.1 and (b) 5.0. A low flux rate of $F=0.04$ has been chosen in both the figures.

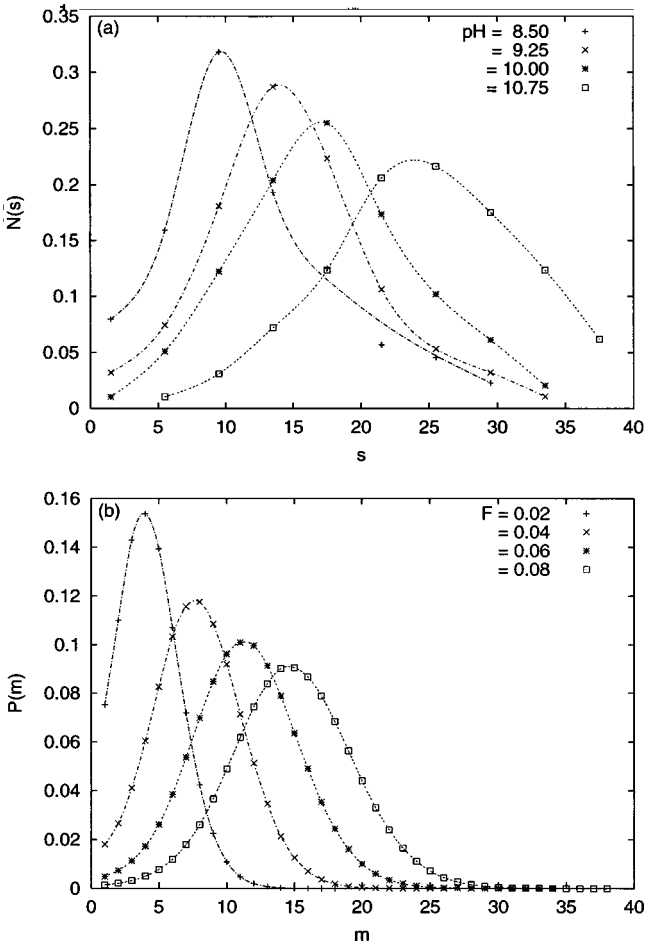


FIG. 2. (a) Particle size distribution of $Pb_{0.5}Fe_{0.5}S$ nanoparticle films for four different values of *p*H of the chemical bath. The lines are a guide to the eye. (b) Mass distribution obtained from simulations for four different values of particle flux $F$ after 500 MCS. The lines are a guide to the eye.

domly occupied sites. At each time step, a particle or a cluster is selected at random and is moved by one lattice unit in a randomly chosen direction. Two clusters aggregate irreversibly on contact. With increasing time the number of clusters decreases and large randomly branched aggregates appear. Typical forms of the diffusion term used in these models are $m^{-1/2}$ [29], $m^{-1}$ [30], and $m^{-\gamma}$ [31]. The fractal dimension of the resulting clusters was the issue of interest in the first two cases while mass distributions for different times were studied in the third case. We on the other hand have an additional adsorption term with relevance to the experiments discussed in Sec. II. Thus in the context of the above models what we have is a nonconserved mass model with point particles.

More realistic models could include further details such as desorption and fragmentation of particles. We will see in Sec. IV that even this simple scenario is capable of describing the robust features of growth in $Pb_{1-x}Fe_xS$ nanoparticles.

## IV. RESULTS AND DISCUSSION

The results of Monte Carlo simulations of our stochastic lattice model with adsorption and diffusion, introduced in the preceding section, are presented here. All simulations have been performed over a two-dimensional discrete lattice of size $250\times250$ with periodic boundary conditions. The data presented were averaged over 1000 initial conditions. At large Monte Carlo time steps (MCS) a complete filing up of the lattice is anticipated with single particle adsorption being the only contributing mechanism toward growth. Since we want both the adsortion and the diffusion moves to contribute to the growth process, we work with low flux rates and refrain from long Monte Carlo runs to ensure a sizable fraction of unoccupied sites.

We first study the role of the diffusion parameter $\gamma$ in the mass distribution $P(m)$ for a flux rate $F$ of 0.04. Figure 1(a) depicts the particle size distribution after 500 (squares) and 1000 (circles) MCS for $\gamma=0.1$. For this value of $\gamma$, the processes of adsorption and diffusion are of a similar strength. The two competing mechanisms yield the steady state single site mass distribution as a time independent power law $P(m)\sim m^{-\tau}$ with the exponent $\tau=1.45\pm0.01$. This observation conforms with the mean field analysis of the Smoluchowski rate equations used to model submonolayer epitaxial growth by Krapivsky *et al.* [20] where they predict $\tau=(3-\gamma)/2$ when $\gamma<1$.

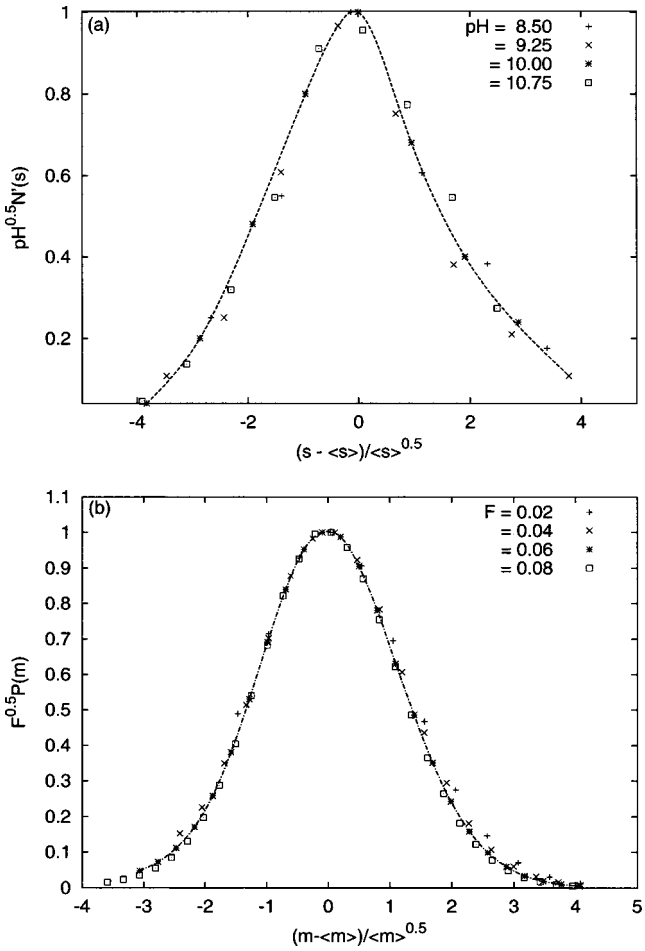


FIG. 3. (a) Scaled experimental data of Fig. 2(a). (b) Scaled numerical data of Fig. 2(b). The dashed lines are guides to the eye.

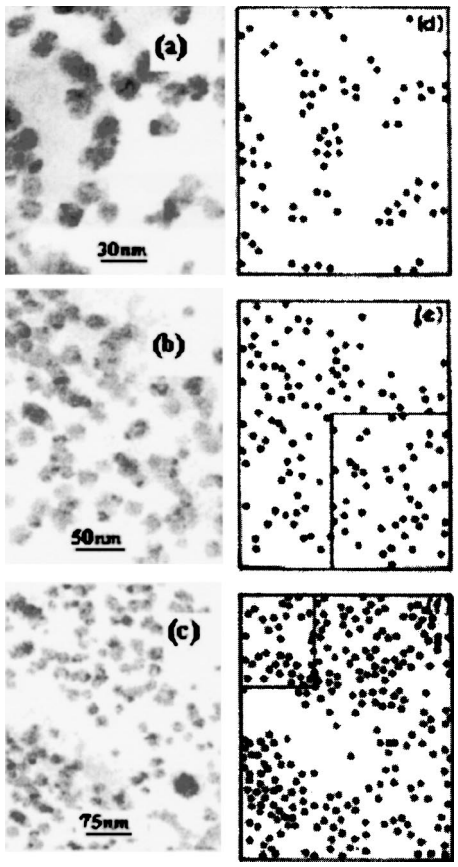


FIG. 4. TEM images of $Pb_{0.5}Fe_{0.5}S$ nanoparticle films for three values of *p*H equal to (a) 9.25, (b) 10.0, and (c) 10.75 of Fig. 2(b). The corresponding point representations are indicated in (d), (e), and (f), respectively. The rectangles in (e) and (f) have been scaled appropriately (see text of Sec. IV) and depicted in Figs. 5(a) and 5(b) below to bring out the aspect of self-similarity in the particle growth process.

For $\gamma \geqslant 1$, a continuous evolution of islands with a peaked mass distribution is anticipated in Ref. [20] in the low coverage limit. We find from our simulations that a signature of the power law behavior persits along with the peaked distribution up to a value of $\gamma \approx 2$. Values of $\gamma$ close to 10 result in a Gaussian distribution, even for very low flux rates, implying that single particle adsorption is the only contributing mechanism toward growth. We choose $\gamma$ to be 5, although the qualitative features of the mass distribution remain unaltered for an approximate window of ±3 around it. The occurrence of the peaked distributions in Fig. 1(b) for 500 (squares) and 1000 (circles) MCS for $\gamma = 5.0$ can be explained as follows. Particle growth is expected until a characteristic (average) particle size governed by $F$ and $\gamma$ is attained, beyond which the increased mass makes diffusion a low probability event. The only contributing mechanism to the growth process is then single particle adsorption. The data also indicate the fraction of unoccupied sites. Since we want both adsorption as well as diffusion processes to be effective mechanisms for particle growth, further data are presented for 500 MCS. The flux rate of course is also an influencing factor, but as mentioned earlier, we work in the regime of low flux rates.

Next we study the dependence of particle size distribution $N(s)$ on the adsorption rate. Figure 2(a) shows $N(s)$ versus $s$ for $Pb_{0.5}Fe_{0.5}S$ nanoparticle films deposited for four values of *p*H = 8.5, 9.25, 10.0, and 10.75 of the chemical bath. Each set of data represents the midpoints of histograms corresponding to particle size distributions for the respective values of *p*H. Correspondingly, Fig. 2(b) is the single site mass distribution $P(m)$ obtained from the simulation for $\gamma = 5.0$ and flux rates $F = 0.02$, 0.04, 0.06, and 0.08. Recalling the correspondence between *p*H and $F$, the data exhibit qualitative similarities with respect to decrease in amplitude, shift in peak position, and broadening of distributions for increasing flux rates.

In conventional growth theories, it is well established that particle size distributions obtained from different adsorption rates can be collapsed onto a single curve when scaled appropriately [15]. We now address this issue in the context of experimental as well as numerical data. Figure 3(a) shows the scaled particle size distributions $N'(s) = N(s)(p\mathrm{H})^{0.5}$ versus $(s - \langle s \rangle)/\langle s \rangle^{0.5}$ Correspondingly, Fig. 3(b) shows the scaled numerical data $P'(m) = P(m)F^{0.5}$ as a function of $(m - \langle m \rangle)/\langle m \rangle^{0.5}$. A comment on the power of $F$ is in order. According to the mean field analysis of Krapivsky *et al.*, the growth rate predominantly goes as $F^{0.333}$ in one dimension and $F^{0.5}$ in two dimensions in the low coverage limit. Recall-

ing that the $Pb_{0.5}Fe_{0.5}S$ nanoparticle films are on a two-dimensional substrate, the scaling in both sets of data is in agreement with the mean field predictions of [20]. The data collapse thus justifies our identification of the *p*H of the chemical bath in the experiments with the impinging flux $F$ in the simulations.

We now interpret the scaling of Fig. 3. Scaling is an indication of self-similarity of particle size distributions with respect to the adsorption rate. This feature can be analyzed more closely from the TEM images of $Pb_{0.5}Fe_{0.5}S$ shown in Figs. 4(a)–4(c) for three values of $p\mathrm{H}=9.25$, 10, and 10.75, respectively. The images will be self-similar if appropriate magnifications of Figs. 4(b) and 4(c) yield images similar to Fig. 4(a) with respect to placement of particles or, alternatively, regions devoid of particles. One problem related to magnification is an inherent enlargement of particles. In order to overcome this, we obtain a point representation of the TEM pictures in the adjacent Figs. 4(d)–4(f). While there is loss of information regarding particle sizes, this representation preserves information regarding density, placement, and regions devoid of particles. After ensuring that the scales in all the figures are the same, the pictures are magnified by a factor $\alpha=(p\mathrm{H}/9.25)^{0.5}$. The assumed definition follows naturally from the scaling function $N'(s)$. The resulting pictures are presented in Figs. 5(a) and 5(b) for $p\mathrm{H}=10$ and 10.75, respectively. The above set of figures along with Fig. 4(d) demonstrate self-similarity in the growth of nanoparticle films of $Pb_{1-x}Fe_xS$ corresponding to different adsorption rates.

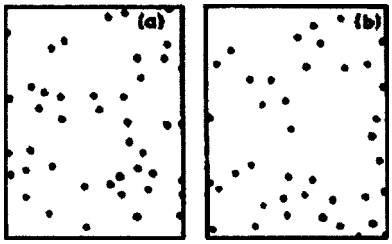


FIG. 5. (a) and (b) are scaled representation of rectangular regions in Figs. 4(e) and 4(f), respectively.

## V. CONCLUSION

In conclusion, we have a simple model involving the basic mechanisms of adsorption and mass dependent diffusion and aggregation to mimic growth of $Pb_{1-x}Fe_xS$ nanoparticle films obtained using a chemical bath deposition technique. The qualitative features of the particle size distributions in deposited films are borne out by the simulations of the proposed model. The distributions for different adsorption rates show a collapse when scaled by the square root of the probability of adsorption in both cases. The scaling represents a self-similarity which is checked using the TEM data of the $Pb_{1-x}Fe_xS$ films obtained with different adsorption rates.

More realistic models could include further details such as desorption and fragmentation of particles to bring further qualitative agreement between experimental and numerical data. In particular, it is of definite interest to include interparticle interactions and study their role in particle growth. It is also of interest verify the distinct distributions resulting by varying the diffusion parameter $\gamma$ in the simulations of depositions of $Pb_{1-x}Fe_xS$ films. It is evident that $\gamma$ is intimately related to the ambient temperature of the bath as well as the substrate. These aspects are being investigated.

## ACKNOWLEDGMENTS

We thank S. Puri and R. Rajesh for suggesting many changes toward improvement of the manuscript. Discussions with S. Krishnamurthy are gratefully acknowledged. We also thank P. Srivastava for a careful reading of the manuscript.

[1] *Kinetics of Ordering and Growth at Surfaces*, NATO Advanced Study Institute, Series B: Physics, edited by M. Legally (Plenum, New York, 1990), Vol. 239.
[2] *Dynamics of Fractal Surfaces*, edited by F. Family and T. Vicsek (World Scientific, Singapore, 1991).
[3] T. Vicsek, *Fractral Growth Phenomena*, 2nd ed. (World Scientific, Singapore, 1992).
[4] *Morphological Organization of Epitaxial Growth and Removal*, edited by Z. Zang and M. G. Legally (World Scientific, Singapore, 1998).
[5] P. Jensen, Rev. Mod. Phys. **71**, 1695 (1999).
[6] J. Y. Sao, *Material Fundamentals of Molecular Beam Epitaxy* (World Scientific, Singapore, 1993).
[7] *Reflection High Energy Electron Diffraction and Reflection Electron Imaging of Surfaces*, NATO Advanced Study Institute, Series B: Physics, edited by P. K. Larsen and P. J. Dobson (Plenum, New York, 1988), Vol. 188.
[8] Y.-W. Mo, J. Kleiner, M. B. Webb, and M. G. Legally, Phys. Rev. Lett. **66**, 1998 (1991).
[9] J. A. Stroscio, D. T. Pierce, and R. A. Dragoset, Phys. Rev. Lett. **70**, 3615 (1993).
[10] J. A. Stroscio and D. T. Pierce, Phys. Rev. B **49**, 8522 (1994).
[11] J. M. Wen, S.-L. Chang, J. W. Burnett, J. W. Evans, and P. A. Thiel, Phys. Rev. Lett. **73**, 2591 (1994).
[12] K. Morgenstern, G. Rosemfeld, B. Poelsema, and G. Comsa, Phys. Rev. Lett. **74**, 2058 (1995).
[13] J. M. Wen, J. W. Evans, M. C. Bartelt, J. W. Burnett, and P. A. Thiel, Phys. Rev. Lett. **76**, 652 (1996).
[14] W. W. Pai, A. K. Swan, Z. Zhang, and J. F. Wendelken, Phys. Rev. Lett. **79**, 3210 (1997).
[15] M. C. Bartelt and J. W. Evans, Phys. Rev. B **46**, 12675 (1992).
[16] P. Jensen, A.-L. Barabasi, H. Larralde, S. Havlin, and H. E. Stanley, Phys. Rev. B **50**, 15316 (1994).
[17] L. Kuipers and R. E. Palmer, Phys. Rev. B **53**, R7646 (1996).
[18] I. Furman and O. Biham, Phys. Rev. B **55**, 7917 (1997).
[19] P. L. Krapivsky and S. Redner, Phys. Rev. E **54**, 3553 (1996).
[20] P. L. Krapivsky, J. F. F. Mendes, and S. Redner, Phys. Rev. B **59**, 15950 (1999).

[21] M. N. Popescu, J. G. Amar, and F. Family, Phys. Rev. B **64**, 205404 (2001).
[22] R. Rossetti, R. Hull, J. M. Gibson, and L. E. Brus, J. Chem. Phys. **83**, 1406 (1985).
[23] R. Thielsch, T. Bhme, R. Reiche, D. Schlfer, H. D. Bauer, and H. Bttcher, Nanostruct. Mater. **10**, 131 (1998).
[24] N. Chestnoy, R. Hull, and L. E. Brus, J. Chem. Phys. **85**, 2237 (1986).
[25] R. K. Joshi and H. K. Sehgal, Nanotechnology **14**, 592 (2003); R. K. Joshi, Aloke Kanjilal, and H. K. Sehgal, *ibid.* **14**, 809 (2003).
[26] S. N. Majumdar, S. Krishnamurthy, and M. Barma, Phys. Rev. Lett. **81**, 3691 (1998); Phys. Rev. E **61**, 6337 (2000); J. Stat. Phys. **99**, 1 (2000).
[27] R. Rajesh, D. Das, B. Chakraborty, and M. Barma, Phys. Rev. E **66**, 056104 (2002).
[28] A. F. Voter, Phys. Rev. B **34**, 6819 (1986).
[29] M. Kolb, R. Botet, and R. Jullien, Phys. Rev. Lett. **51**, 1123 (1983).
[30] P. Meakin, Phys. Rev. Lett. **51**, 1119 (1983).
[31] T. Vicsek and F. Family, Phys. Rev. Lett. **52**, 1669 (1984).